PROCEEDINGS OF SPIE

SPIEDigitalLibrary.org/conference-proceedings-of-spie

Three-dimensional monochromatic light field synthesis with a deflectable mirror array device

Erdem Ulusoy
Vladislav Uzunov
Levent Onural
Haldun M. Ozaktas
Atanas Gotchev

SPIE.

Three-Dimensional Monochromatic Light Field Synthesis with a Deflectable Mirror Array Device

Erdem Ulusoy[1], Vladislav Uzunov[2], Levent Onural[1],
Haldun M. Ozaktas[1] and Atanas Gotchev[2]

[1]Bilkent University, Department of Electrical and Electronics Engineering, TR-06800, Ankara, Turkey

[2]Tampere University of Technology, Institute of Signal Processing, FIN-33101, Tampere, Finland

ABSTRACT

We investigated the problem of complex scalar monochromatic light field synthesis with a deflectable mirror array device (DMAD). First, an analysis of the diffraction field produced by the device upon certain configurations is given assuming Fresnel diffraction. Specifically, we derived expressions for the diffraction field given the parameters of the illumination wave and the tilt angles of the mirrors. The results of the analysis are used in later stages of the work to compute the samples of light fields produced by mirrors at certain points in space. Second, the light field synthesis problem is formulated as a linear constrained optimization problem assuming that mirrors of the DMAD can be tilted among a finite number of different tilt angles. The formulation is initially developed in the analog domain. Transformation to digital domain is carried out assuming that desired fields are originating from spatially bounded objects. In particular, we arrived at a $\mathbf{Dp} = \mathbf{b}$ type of problem with some constraints on $\mathbf{p}$, where $\mathbf{D}$ and $\mathbf{b}$ are known, and $\mathbf{p}$ will be solved for and will determine the configuration of the device. This final form is directly amenable to digital processing. Finally, we adapt and apply matching pursuit and simulated annealing algorithms to this digital problem. Simulations are carried out to illustrate the results. Simulated annealing performs successful synthesis when supplied with good initial conditions. However, we should come up with systematic approaches for providing good initial conditions to the algorithm. We do not have an appropriate strategy currently. Our results also suggest that simulated annealing achieves better results than MP. However, if only a part of the mirrors can be used, and the rest can be turned off, the performance of MP is acceptable and it turns out to be stable for different types of fields.

Keywords: Light Field Synthesis, Deflectable Mirror Array Device, Fresnel Diffraction, Linear Constrained Optimization Problem, Matching Pursuit Algorithm, Simulated Annealing Algorithm

1. INTRODUCTION

In this work we consider the problem of complex scalar monochromatic light field synthesis with a deflectable mirror array device (DMAD) and we deal with the associated signal processing. The DMAD is a reflection-mode spatial light modulator (SLM), which consists of a two-dimensional array of square shaped identical micro-mirrors. The mirrors can be tilted along their diagonal axes. The deflection of each mirror can be controlled separately. One of the most widely used practical DMADs is the digital micromirror device (DMD) developed by Texas Instruments.[1] This device comprises a large number of mirrors, typically in the order of a million mirrors per chip. This device has been used for the synthesis of high quality two-dimensional color images in digital video display systems.[2] It has also been occasionally used in holographic applications. In particular, its employment in generation of holographic stereograms was suggested,[3] and its usage in digital holographic interferometry to synthesize binary amplitude holograms was proposed.[4]

Here we concentrate on the usage of DMADs to synthesize desired monochromatic light fields within a spatial volume of interest. Piestun and Shamir[5] formulate the general light field synthesis problem as the optimization of device configurations for the purpose of achieving the most successful creation of a desired light field within

This work is supported by EC within FP6 under Grant 511568 with acronym 3DTV.

Photon Management II, edited by John T. Sheridan, Frank Wyrowski, Proc. of SPIE Vol. 6187, 61871J, (2006) · 0277-786X/06/$15 · doi: 10.1117/12.668542

a region in space and in time. Our formulation is similar to theirs. In our case, light fields can be synthesized by appropriately tilting the mirrors on the DMAD and illuminating the device with coherent laser light. The light which is reflected from the mirrors will propagate to approximate the intended light field within the target volume (Fig. 1). Since we posed our problem as the synthesis of monochromatic light fields, time dimension is irrelevant to us. We will basically try to replicate the phasor of a given monochromatic field.

Therefore, given the desired field, the key problem is the determination of the tilt angles of the mirrors accordingly. Therefore it falls in the framework of combinatorial problems. In some applications, it may be the case that this inverse problem should be solved in a fast manner compatible with real-time operation. However, the problem has a very high dimensionality due to the large number of mirrors present on the device. Hence, solving this problem is a challenging task that requires the usage of both accurate and fast combinatorial optimization algorithms. An attractive candidate is the simulated annealing algorithm.[6,7] Its major advantage over other methods is an ability to avoid becoming trapped at local minima. The algorithm employs a random search which not only accepts changes that decrease objective function, but also some changes that increase it with time decaying probability. Another fast algorithm that comes from the field of signal representation is the matching pursuit algorithm.[8] It is a greedy strategy for signal approximation by a linear combination of waveforms, iteratively selected from a large collection. This algorithm can be easily adapted to the problem at hand by restricting the possible values of the coefficients in the linear combination.

Below, we first provide an analysis of the field produced by this device in sec. 2. Up to a point, we summarize the results we derived in an earlier work.[9] We also extend the analysis assuming Fresnel diffraction. Second, we pose the light field synthesis problem as a linear constrained optimization problem in sec. 3. Initially, the problem is posed in the analog domain. The developed framework is independent of particular digitization schemes. Later, assuming that fields to be synthesized are arising due to diffraction from spatially bounded objects, we build up a digital optimization problem on top of the analog optimization problem. This problem can directly be attacked on a digital computer. Finally, we describe the adaption and application of matching pursuit and simulated annealing algorithms to solve this digital optimization problem, respectively in sec. 4.1 and sec. 4.2. We test our formulations and illustrate our results through a number of computer simulations, which we describe in sec. 4.3. Our conclusions are stated in sec. 5.

2. ANALYSIS OF LIGHT FIELD GENERATED BY A DMAD

In this section, we firstly summarize the results of one of our earlier works .[9] In that work, there is an analysis of the light field produced by a DMAD given the tilt angles of the mirrors on the device. However, the results were not specialized for a specific diffraction kernel. Here, we secondly extend the results of that previous analysis for the case of Fresnel diffraction.

We will express the light field produced by the device upon illumination by a plane wave under a certain configuration with respect to the coordinate system shown in Fig. 2. We favored this coordinate system because the mirrors are tilted along their diagonal axes. By this choice, we expect to obtain more manageable expressions at the end. In this coordinate system, tilt axes of mirrors are parallel to y-axis. The mirrors of the DMAD can be indexed with a column vector $\mathbf{i} = \begin{bmatrix} m & n \end{bmatrix}^T$ with $m, n \in \mathcal{Z}$, such that the $\mathbf{i}$'th mirror is centered around:

$$\mathbf{T}_{\mathbf{i}} = \begin{bmatrix} x_c \\ y_c \\ 0 \end{bmatrix} = \left(W\sqrt{2} + \frac{L\sqrt{2}}{2} \right) \begin{bmatrix} -1 & 1 \\ 1 & 1 \\ 0 & 0 \end{bmatrix} \mathbf{i} \tag{1}$$

where $2W$ is the width of the mirrors and L is the length of the spacing between the mirrors.

Let the device be illuminated by an incident plane wave whose functional representation in the coordinate system described above is given by $\exp\left\{ j\frac{2\pi}{\lambda}\kappa^T\mathbf{x} \right\}$. Here, $\mathbf{x}$ is the position vector given by $\mathbf{x} = \begin{bmatrix} x & y & z \end{bmatrix}^T$ and κ is the direction cosines vector of the plane wave given by $\kappa = \begin{bmatrix} \alpha & \beta & \gamma \end{bmatrix}^T$ satisfying the constraint $\alpha^2 + \beta^2 + \gamma^2 = 1$. This incident plane wave will hit the mirrors, and it will be reflected back by each of them. Let us in particular denote the functional representation of the field reflected from the $\mathbf{i}$'th mirror by $u_\kappa^{(\mathbf{i},\theta_\mathbf{i})}(\mathbf{x})$ with respect our coordinate system, assuming that the mirror is tilted by an angle $\theta_\mathbf{i}$ in clockwise direction around its

axis of rotation. Note that the dependence of the field on the direction of the incident plane wave is also stressed through inclusion of the κ parameter to the representation. Then, the total field reflected from the DMAD can be obtained by superposing the individual fields reflected from the mirrors as:

$$u(\mathbf{x}) = \sum_{\mathbf{i}} u_{\kappa}^{(\mathbf{i},\theta_{\mathbf{i}})}(\mathbf{x}) \tag{2}$$

Turning our attention back to the individual fields, $u_{\kappa}^{(\mathbf{i},\theta_{\mathbf{i}})}(\mathbf{x})$ is given as:

$$u_{\kappa}^{(\mathbf{i},\theta_{\mathbf{i}})}(\mathbf{x}) = \exp\left\{ j\frac{2\pi}{\lambda}\kappa^T \mathbf{T}_{\mathbf{i}} \right\} \psi_{\mathbf{R}_{\theta_{\mathbf{i}}}\kappa}\left(\mathbf{R}_{\theta_{\mathbf{i}}}(\mathbf{x} - \mathbf{T}_{\mathbf{i}})\right) \tag{3}$$

where $\mathbf{T}_{\mathbf{i}}$ is the matrix given by Eq. 1, $\mathbf{R}_{\theta}$ is given as:

$$\mathbf{R}_{\theta} = \begin{bmatrix} \frac{1}{\sqrt{2}}\cos\theta & \frac{1}{\sqrt{2}} & \frac{1}{\sqrt{2}}\sin\theta \\ -\frac{1}{\sqrt{2}}\cos\theta & \frac{1}{\sqrt{2}} & -\frac{1}{\sqrt{2}}\sin\theta \\ -\sin\theta & 0 & \cos\theta \end{bmatrix} \tag{4}$$

and the six parameter function $\psi_{\kappa}(\mathbf{x})$ is given as:

$$\psi_{\kappa}(\mathbf{x}) = \psi_{\left[\begin{array}{ccc}\alpha & \beta & \gamma\end{array}\right]^T}\left(\left[\begin{array}{ccc} x & y & z \end{array}\right]^T\right) = h_z(x,y) \otimes_{x,y} \text{rect}\left(\frac{x}{2W}\right)\text{rect}\left(\frac{y}{2W}\right)\exp\left\{ j\frac{2\pi}{\lambda}(\alpha x + \beta y)\right\} \tag{5}$$

Here, $h_z(x,y)$ denotes the impulse response of free space propagation system and $\otimes_{x,y}$ denotes 2D convolution in the x and y coordinates.

We refer to Fig. 3 to explain the function defined in Eq. 5 in more detail. In this figure, as seen, there is a single square shaped mirror of width $2W$, and this mirror is placed in a coordinate system such that its aperture can be described by $\text{rect}\left(\frac{x}{2W}\right)\text{rect}\left(\frac{y}{2W}\right)$. Also, this mirror is illuminated by a plane wave, which is represented by $\exp\left\{ j\frac{2\pi}{\lambda}\kappa^T\mathbf{x}\right\} = \exp\left\{ j\frac{2\pi}{\lambda}(\alpha x + \beta y + \gamma z)\right\}$. Hence, the field on the mirrors aperture becomes $\text{rect}\left(\frac{x}{2W}\right)\text{rect}\left(\frac{y}{2W}\right)\exp\left\{ j\frac{2\pi}{\lambda}(\alpha x + \beta y)\right\}$. This function can be convolved with $h_z(x,y)$ to arrive at the description of the field that is reflected from the mirror. Since $\psi_{\kappa}(\mathbf{x})$ is obtained exactly in the same way as suggested by Eq. 5, $\psi_{\kappa}(\mathbf{x})$ actually represents the reflected field in the problem depicted in Fig. 3.

The equations derived up to this point are valid regardless of the choice for the diffraction kernel $h_z(x,y)$. Actually, only the $\psi_{\kappa}(\mathbf{x})$ function of Eq. 5 is influenced by the choice of the diffraction kernel. In the rest of this section, we will derive explicit expressions for this function under the Fresnel approximation for free-space diffraction. The Fresnel kernel for free-space diffraction is given as[10]:

$$h_z(x,y) = \frac{e^{jkz}}{j\lambda z} e^{j\frac{k}{2z}(x^2+y^2)} \tag{6}$$

Above, we pointed the connection between the problem depicted in Fig. 3 and $\psi_{\kappa}(\mathbf{x})$. Therefore, to solve for $\psi_{\kappa}(\mathbf{x})$, we have to solve the problem in Fig. 3 for arbitrary values of κ, i.e. for arbitrary illumination directions, assuming Fresnel diffraction. In the fourth chapter of his book,[10] Goodman solves this problem for the case of normally incident illumination ($\alpha = \beta = 0$, $\gamma = -1$). In particular, he achieved the following result:

$$\psi_{\left[\begin{array}{ccc} 0 & 0 & -1 \end{array}\right]^T}\left(\left[\begin{array}{ccc} x & y & z \end{array}\right]^T\right) = \frac{e^{jkz}}{j} I(x)I(y) \tag{7}$$

where

$$I(x) = \frac{1}{\sqrt{\lambda z}}\int_{-W}^{W} \exp\left\{ j\frac{\pi}{\lambda z}(x-\zeta)^2\right\} d\zeta \tag{8}$$

Here, as previously declared, $2W$ is the width of the mirrors. Eq. 8 can be simplified further by setting

$$\alpha_1 = -\sqrt{\frac{2}{\lambda z}}(W + x) \tag{9}$$

$$\alpha_2 = \sqrt{\frac{2}{\lambda z}}(W - x) \tag{10}$$

Using the new variables above, Eq. 8 can be rewritten as

$$I(x) = \frac{1}{\sqrt{2}} \left\{ [C(\alpha_2) - C(\alpha_1)] + j \, [S(\alpha_2) - S(\alpha_1)] \right\} \tag{11}$$

where $C(z)$ and $S(z)$ are the familiar frequently encountered and tabulated Fresnel integrals:

$$C(z) = \int_0^z \cos\left(\frac{\pi t^2}{2}\right) dt \tag{12}$$

$$S(z) = \int_0^z \sin\left(\frac{\pi t^2}{2}\right) dt \tag{13}$$

To extend these results to the case of oblique illumination with small incidence angle (for general α, β, γ satisfying $\alpha^2 + \beta^2 + \gamma^2 = 1$, and α, β sufficiently small so that Fresnel approximation is valid) we essentially went through a procedure similar to that outlined by Goodman,[10] and arrived at the following explicit formula for $\psi_\kappa(\mathbf{x})$:

$$\psi_{\left[\begin{array}{ccc}\alpha & \beta & \gamma\end{array}\right]^T}\left(\left[\begin{array}{ccc}x & y & z\end{array}\right]^T\right) = \frac{e^{jkz}}{j} \exp\left\{ j \frac{\pi}{\lambda z} \left(2\alpha z x - \alpha^2 z^2\right) \right\} I(x - \alpha z) \exp\left\{ j \frac{\pi}{\lambda z} \left(2\beta z y - \beta^2 z^2\right) \right\} I(y - \beta z) \tag{14}$$

where $I(x)$ is given by Eq. 8 as before.

3. LINEAR CONSTRAINED OPTIMIZATION PROBLEM FORMULATION

Our main intention is to synthesize monochromatic light fields with a DMAD in a space region of interest to the best extent. As explained in detail in sec. 1, to synthesize a desired complex light field to the best extent, we must determine the optimum tilt angles for the mirrors. Therefore, we should develop a procedure to convert the specifications of the desired light field to these optimum tilt angles. In this section, we formulate the problem of complex monochromatic light field synthesis with a DMAD as a linear constrained optimization problem. A lot of readily available optimization algorithms exist for this class of problems. For the rest of this paper, we assume that the mirrors on the DMAD we work with can be tilted to a finite number of discrete tilt angles, rather than being continuously tunable.

For convenience, we slightly change the notation of the previous section. Let us assume that our DMAD consist of $M \times N$ ($M, N \in \mathcal{Z}^+$) micro-mirrors and each micro-mirror can be tuned to $S \in \mathcal{Z}^+$ different discrete tilt angles. Since the mirrors are finite in number, let us adopt a one-dimensional indexing scheme for the mirrors this time, reserving the letter j for the mirror index, such that $j \in \mathcal{Z}$ and $1 \leq j \leq M \times N$. Let $u_{j_s}(\mathbf{x})$ denote the field generated by j'th mirror when it is tilted to s'th position ($s \in \mathcal{Z}$, $1 \leq s \leq S$). Finally, let $b(\mathbf{x})$ represent the desired light field.

With this new notation, the total light field produced by the DMAD can be expressed in the following form:

$$u(\mathbf{x}) = \sum_{j=1}^{M \times N} \sum_{s=1}^{S} p_{j_s} u_{j_s}(\mathbf{x}) \tag{15}$$

This expression represents the field for a fixed configuration of the device (i.e. the configuration does not change in time) such that the tilt angles for the entire DMAD have been specified. At first glance, this expression seems to be a linear combination of all individual fields generated by the mirrors. However, there are several constraints associated with this linear combination due to the nature of the device. In particular, all the possible fields $u_{j_s}(\mathbf{x})$ cannot be present in this linear combination with nonzero coefficients simultaneously. Only one of the S fields produced by each mirror can be contributing to the total field, since each mirror can be tilted to a single position at any time. On the other hand, each mirror on the chip will in any case be tilted in one of the

S angles in a fixed manner, so will inevitably be producing one of the S fields. All of these remarks imply that in Eq. 15, for each j, strictly one of the coefficients p_{j_s} is one and the others are zero.

Therefore, Eq. 15 is actually a constrained linear combination of the individual fields produced by each mirror. Remember that given $b(\mathbf{x})$ (the desired field), our aim is to determine the set of optimum tilt angles for the mirrors. In other words, for all j, we want to find out the best selections for the nonzero and unity coefficients p_{j_s}, such that $b(\mathbf{x})$ is synthesized to the best extent. At this point, we have set the light field synthesis problem as a linear constrained optimization problem in the analog domain.

Although we have a well-defined optimization problem in the analog domain, we will most likely have to solve this problem in digital domain. Therefore, we have to transform the analog problem into an equivalent digital problem. For this purpose, the first step is the digitization of the information present in the analog light fields $u_{j_s}(\mathbf{x})$ and $b(\mathbf{x})$. There may be various strategies for this task, each of which makes sense under different assumptions and approximations. Here, we base our digitization strategy on the assumption that the light fields we wish to synthesize propagate from spatially bounded objects. We believe this is reasonable in real-world situations. When the Fresnel approximation is considered for diffraction, light fields emerging from spatially bounded objects can be represented fully by their samples taken at finite rates.[11,12] In the case of arbitrary spatially bounded objects, the number of samples required to fully characterize the diffraction fields might be infinite. In our work, we further assume that a finite number of samples is enough to characterize the fields. We assume that all the fields we wish to synthesize are fully determined by their samples taken at a set of R ($R \in \mathcal{Z}^+$) predetermined space locations. Thus, we can represent $u_{j_s}(\mathbf{x})$ and $b(\mathbf{x})$ by vectors $\mathbf{u_{j_s}}$ and $\mathbf{b}$ respectively. Both $\mathbf{u_{j_s}}$ and $\mathbf{b}$ are of size $R \times 1$.

Finally, we get the following matrix equation as a digital description of our light field synthesis problem:

$$\mathbf{Dp} = \mathbf{b} \tag{16}$$

In the above equation,

- Vector $\mathbf{b} \in \mathcal{C}^{R\times 1}$ represents the given field as stated before.
- $\mathbf{D} \in \mathcal{C}^{(M\times N\times S)\times R}$ represents the behavior of the device. Each column of $\mathbf{D}$, which is of size $R \times 1$, corresponds to the samples of one of the individual fields produced by one of the mirrors on the device. Specifically, the $\{(j-1)\times S + s\}$th column of $\mathbf{D}$ is $\mathbf{u_{j_s}}$.
- $\mathbf{p} \in \mathcal{R}^{(M\times N\times S)\times 1}$ generates the constrained linear combination of the columns of $\mathbf{D}$, as previously stated through Eq. 15. We seek to solve for this vector actually, which will dictate the choice of tilt positions of the mirrors. The already discussed constraints of the problem reduce the set of possible values for this vector. In particular, the following requirements should be fulfilled: $\mathbf{p}$ is such that for all $k \in \mathcal{Z}$, $1 \le k \le M \times N$; the sub-vector $\mathbf{p}\,[(k-1)\times S + 1 : k \times S]$ is equal to a column of the $S \times S$ identity matrix. Each of these sub-vectors actually determine the configuration of a single mirror. The nonzero element within the sub-vector will correspond to the tilt angle selected for that mirror.

At last, we achieved a discretized linear constrained optimization problem. The problem can be attacked on a digital computer in this form. A myriad of algorithms exist for this type of problems, such as constrained least squares, matching pursuit or simulated annealing, and they can be applied to solve for the optimum tilt angles (the vector $\mathbf{p}$) given the desired field (the vector $\mathbf{b}$) and the specifications of the device (the matrix $\mathbf{D}$).

4. APPLICATION OF MATCHING PURSUIT AND SIMULATED ANNEALING ALGORITHMS

Having put our optimization problem in a suitable format for digital processing, now it is time to adapt and apply solution algorithms. For this purpose, here we consider matching pursuit and simulated annealing algorithms, and report our simulation results. First, we give a brief introduction to these algorithms.

4.1. Matching Pursuit Algorithm

The light field synthesis problem, as formulated by Eq. 15, can be formally interpreted as a signal representation problem. The desired light field $u(\mathbf{x})$ can be considered as a signal that has to be represented by linear combination of waveforms, selected from a dictionary $\mathbf{D}$. These waveforms can be the light fields $u_{j_s}(\mathbf{x})$ generated by the mirrors of the DMAD. Respectively, p_{j_s} are the coefficients in the representation. The difference in our problem is the restrictions on these coefficient that were imposed in subsection 3. Since we deal with practical light fields that cannot be always synthesized exactly by the DMAD, their approximate representation can be stated as

$$u(\mathbf{x}) = \sum_{j=1}^{m} \sum_{s=1}^{S} p_{j_s} u_{j_s}(\mathbf{x}) + R^{(m)}(\mathbf{x}), \tag{17}$$

where $R^{(m)}(\mathbf{x})$ is the signal residual after synthesis by $m < M \times N$ dictionary elements. Mallat and Zhang[8] have discussed a general method for such approximate decomposition that addresses the sparsity issue directly. Matching pursuit (MP) is a recursive, adaptive algorithm that builds up the signal representation one element at a time, picking the most contributive element at each step. Starting from an initial residual $R^{(0)}(\mathbf{x}) = u(\mathbf{x})$, the element chosen at the jth step is the one which minimizes $\|R^{(j)}(\mathbf{x})\|$ as defined in (17). The residual at stage j is given by $R^{(j)}(\mathbf{x}) = R^{(j-1)}(\mathbf{x}) - p_{j_s} u_{j_s}(\mathbf{x})$.

The MP approach works well for many types of signals. It has been shown to be especially useful for extracting structure from signals which consist of components with widely varying time-frequency localizations.[8] When stopped after a few steps, it yields an approximation using only a few atoms. The algorithm selects the dictionary elements one by one, resulting in a local optimization. Therefore, in certain cases it might choose wrongly in the first few iterations and end up spending most of its time correcting for any mistakes made in the first few terms. This results in an algorithm that may end up far from the global optimal solution.

Despite of this drawback, MP is a very attractive choice since it is a fast search procedure. This is necessary when one has to deal with DMADs consisting of thousands of mirrors. Another advantage in comparison with most of the traditional optimization methods is that MP can be easily modified to adopt the constraints on the coefficients p_{j_s}. This modification is outlined below.

- initialize $R^{(0)}(\mathbf{x}) = u(\mathbf{x})$
- for $j = 1$ to MN
  - (a) go through all the mirrors and their positions and pick the most contributive one: $\{i, s\} = \arg\min_{i,s} \|R^{(j-1)}(\mathbf{x}) - p_{i_s} u_{i_s}(\mathbf{x})\|$
  - (b) update residual $R^{(j)}(\mathbf{x}) = R^{(j-1)}(\mathbf{x}) - p_{i_s} u_{i_s}$
- end

The orthogonality between the light fields reflected from each mirror of the DMAD is highly dependent on the chosen sampling grid. Therefore, the dictionary elements for our specific case are not necessarily orthogonal and the MP algorithm is expected to show its local optimality behavior. This raises the question of whether higher-order optimizations may be of benefit. To clarify this need some experiments were done also with a "second-order" matching pursuit (MP2). It follows essentially the same strategy as described above. The difference is that at step (a), instead of the most contributive mirror, a combination of the two most contributive mirrors is found. At step (b) the joint contribution of these two mirrors is subtracted from the residual. It should be noted that the complexity of the search for pairs of most contributive mirrors increases to $O((M \times N)^3)$ in comparison to $O((M \times N)^2)$ in the case of first order matching pursuit.

4.2. Simulated Annealing Algorithm

Simulated annealing is a well-known and frequently used optimization algorithm.[6,7] Since it is widely used, we will directly present its application to our problem. Basically, in our case the algorithm starts with an initial configuration of the mirrors, and we hope to eventually arrive at a state such that the desired field is replicated to a satisfactory extent. In our experiments, as the distance metric, we use the total mean-squared error; and we use the reciprocal of this quantity as the quality measure to assess the level of success within the reconstruction. We go over all the mirrors sequentially. When we are handling a specific mirror during the iterations, we firstly calculate the current value of quality measure, Q_1. Then, we switch the current tilt angle of the mirror arbitrarily to one of the remaining options, and calculate the new value of the quality measure, Q_2. We calculate the ratio between these two quantities, $r = \frac{Q_2}{Q_1}$, which signals the effect of the change that is attempted. If the results improve with this modification ($r > 1$), the state of the mirror is updated to the new tilt position. On the other hand, if there is a deterioration in the results ($r \leq 1$), the change is performed with a probability of $rT(t)$, where $T(t)$ is a time-dependent weighting function. As stated before, all the mirrors on the chip will be experimented sequentially with this simple test, and their stated will be altered appropriately if necessary. Usually, within the overall run, there will be several passages over the entire chip. Remembering from previous sections that we had $M \times N$ mirrors, if the number of passages over the entire chip is $K \in \mathcal{Z}^+$, there will be a total of $K \times M \times N$ mean squared error computations and comparisons during execution of the algorithm.

The weighting function is the essential part of the algorithm for the purpose of simulating the annealing part. Specifically, when the algorithm is running, this function has high values during the earlier stages, while its value decreases as the number of iterations increase. Since it directly influences the decision on whether a change will be made under degradation of results or not, the interpretation of its effect is as follows: at the beginning, even if results become worse, changes are allowed and enhanced. The aim here is to prevent the algorithm to converge to a local optimum, but rather provide it with a chance to step on a path through which it can arrive at the global optimum. Towards the end of the algorithm though, changes resulting in spoilage are barely allowed, this time to prevent the algorithm from getting out of the road that leads to the global optimum.

In our simulations, we selected $K = 40$. As for the weighting function, we used $T(t) = \exp\left\{-\frac{t}{4 \times M \times N}\right\}$. When the j'th mirror was processed for the k'th ($k \in \mathcal{Z}$, $1 \leq k \leq K$) time, this function was evaluated at $t = (k-1) \times M \times N + j$, and the obtained value is assigned as the weighting factor to be used during the operations.

4.3. Simulation Results

We have carried out several simulations to illustrate and verify the usefulness of our formulations and results developed in the previous sections.

In our simulations, we represented the target field by its samples taken uniformly on a square planar patch residing in front of the DMAD. Through optimization algorithms, we tried to configure the DMAD to reconstruct these samples with minimum error. Our error criteria is the mean squared error of the difference signal between the samples of the original and reconstructed fields.

Our convention for exact placement of the sampling patch relative to the DMAD is illustrated in Fig. 4. The coordinate system here is the same as in Fig. 2. First, we calculated the dimensions of the square region on the $z = 0$ plane in which the DMAD exactly fits. This region is shown as R_1 in Fig. 4, with dimensions $d_1 \times d_1$. The distance of the sampling patch R_2 to the DMAD is taken to be $z = d_1$, while the dimensions of the sampling patch are chosen as $d_2 = 0.75d_1$.

The simulations were carried out separately for two DMADs of sizes 25×25 and 71×71. In both cases, the mirrors were $16\mu m \times 16\mu m$ in size, and they could be tilted to -12,0 and 12 degrees (their axes of rotation is parallel to the y-axis in Fig. 4) and the interspacing between the mirrors was $1\mu m$. For the case of 25×25 DMAD, all the light fields were represented by 11×11 uniformly distributed samples on the sampling patch. The distance of the patch to the mirrors was $z = 300\mu m$, while the sampling interval in both x and y directions were $dx = dy = 45\mu m$. When we used instead the 71×71 DMAD, the sampling patch consisted of 25×25 uniformly distributed samples, the distance of the patch to the mirrors turned out to be $z = 853\mu m$, while the sampling intervals became $dx = dy = 53\mu m$.

In all the experiments, the DMADs were illuminated by normally incident plane waves of wavelength $\lambda = 633nm$. To arrive at the format suggested by Eq. 16, we firstly prepared the matrix $\mathbf{D}$ by computing the samples of the fields produced by mirrors of the chip on the sampling patch. We made extensive use of the formulas developed in sec. 2 for that purpose. In our experiments with the 25×25 DMAD, $\mathbf{D}$ had a size of 121×1875. The row size follows since the sampling patch consists of 11×11 samples, resulting in a total of 121 samples. The column size is obtained as $675 \times 3 = 1875$ since there are a total of 625 mirrors and each mirror can be tilted to three different angles. In the case of the 71×71 device, the size of $\mathbf{D}$ became 625×15123.

With both the 25×25 and 71×71 DMADs, we conducted the simulations for two target fields. One of these fields was randomly selected within the range space of the device, so that the optimization problem had an exact solution. The other one was chosen to be circle function. We tried to reconstruct the samples of this circular field. In this case, we tried to find out the configuration that produced the closest set of samples to the original field in minimum mean-squared sense. The performance of the proposed algorithms was evaluated with the percentage mean squared error error. It is computed by dividing the mean square error of reconstruction to the total energy of the original samples, and multiplying the result by 100.

In the first experiment a 25×25 DMAD was used to to synthesize a field which was in its range space, where the optimal tilt positions of the mirrors were found by using first- and second-order matching pursuit algorithms. Fig. 5 shows the progress of the percentage error along with the number of iterations. (Note that in the case of matching pursuit algorithm, the total number of iterations equal the total number of mirrors.) The dashed curve is associated with first-order matching pursuit, while the solid one shows the error when second-order matching pursuit is used. These curves illustrate the performance of MP as a fast approximation strategy using minimal number of dictionary elements. Both versions of the algorithm arrive at an approximate solution - 0.8% and 0.5% error for first and second order matching pursuit respectively. In both cases, this lowest value is reached after the 400th iteration - less than the total number of mirrors. After a good approximate solution has been found with minimum number of mirrors, adding more mirrors increases the error when they are combined with the mirrors selected so far. This due to the fact that the expansion coefficients in 17 are restricted only to unity and the portion of reflected light from a mirror cannot be controlled to minimize the error further. On the contrary, when it is strictly unity it degrades the approximation when combined with the other mirrors. Indeed, the final errors yielded by the algorithms were 5.5% and 4.3%. Another important observation is that for any number of mirrors the second order MP leads to lower error. These suggests that the use of global optimization algorithm will be of benefit.

We also tried to reconstruct the field above using simulated annealing. This algorithm and the solution it converges is inevitably influenced by the initial estimate begun with. At first, we ran the algorithm a hundred times in which for each run we randomly selected an initial configuration, and among the hundred results, we looked at the most satisfactory one. In this trial, we were able to recover the exact configuration that produced the input field. However, in most of the trials the algorithm is stuck in a local minimum and finds only an approximate solution. Therefore we lack a systematic approach for selection of the initial conditions which will lead in most of the cases to the global optimum.

For the 25×25 DMAD, another group of simulations were performed when the target field had a circular distribution of $1.5circ\left(\frac{\sqrt{\left(\frac{x}{dx}\right)^2+\left(\frac{y}{dy}\right)^2}}{2}\right)$. This field was not necessarily in the range space of the device. Results with first- and second-order matching pursuit algorithms are plotted in Fig. 5. Still the performance of second-order algorithms is better - the errors are 1.0% (MP) and 0.7% (MP2) percent during the iterations. However, this time the final errors produced by the algorithms had significantly intolerable values - 78.2% (MP) and 74.2% (MP2). We also applied simulated annealing. Firstly, similar to the previous case, we initiated the algorithm a hundred times with randomly selected initial conditions, and searched for the best result. Via this algorithm, the target field was reconstructed up to an error of 13.3%. This shows that if only an approximate solution is theoretically possible, MP is superior to simulated annealing as a greedy algorithm that minimizes the error without trying to recover the underlying structure.

The same sequence of simulations, with some minor changes, were applied to the 71×71 DMAD. We firstly tried to regenerate a field within the range space. This time, due to its high computational complexity, we avoided the application of second-order matching pursuit, but concentrated only on the first-order version. The

propagation of error is demonstrated in Fig. 7. The curve is similar in shape to that in the previous experiments. The final value of the error is 8.8% while the minimum value reached is 0.7%. On the other hand, we observed that when several random initial conditions were applied, simulated annealing recovered the field perfectly. Secondly, we tried to synthesize a circular field distribution of $1.5circ\left(\frac{\sqrt{\left(\frac{x}{dx}\right)^2+\left(\frac{y}{dy}\right)^2}}{2}\right)$. The error curve of first-order matching pursuit algorithm is plotted in Fig. 8. Similar to the counterpart of this simulation for the case of 25×25 DMAD, the final error is unacceptably high (46.5%) in spite of the very low value (0.7%) the error reaches during the iterations. We also applied simulated annealing a hundred times with different initial conditions each time. The best reconstruction we obtained is shown in Fig. 9, while the corresponding error versus iteration number curve is plotted in Fig. 10. (Note that in the case of simulated annealing, the total number of iterations is equal to the multiplication of the total number of mirrors and the total number of passes over the entire device.) The final error is 5.8%.

Consideration of results leads us to the following observations: We infer from the experiments in which the desired field is within the range space of the DMAD that the simulated annealing algorithm is able to perform perfect reconstruction (given good initial conditions). However, we lack a systematic and quick approach to supply good initial estimates that would enable convergence to the global optimum. Another alternative might be to search for parameters of simulated annealing that would yield better results. Our choices here were based on experimental trials instead of more systematic approaches, so they may not be optimal. On the other hand, when considered on its own, the matching pursuit algorithm produces high error values at the end despite the fact that the error goes very low during the iterations. As explained above this is due to the restriction for the coefficients in the expansion 17. However, the experiments with circular fields suggest that the performance of MP does not depend on whether the desired field is theoretically reproducible by the DMAD. Moreover, the convergence time may be very short. Under the assumption that only part of the mirrors can be used to synthesize the field the performance of the matching pursuit approach is acceptable, and the algorithm itself might turn out to be very handy.

5. CONCLUSION

In this work, we addressed the problem of complex monochromatic light field synthesis with a deflectable mirror array device(DMAD). With their large number of degrees of freedom, DMADs are promising spatial light modulators to be used in light field synthesis applications, but they raise challenging inverse problems: finding the optimal position of the mirrors of the DMAD is a difficult optimization problem. The major contribution of this work is the formulation of the problem as a constrained linear optimization problem which can be numerically solved in a fast manner by using any of the dozens of readily existing algorithms for such problems. Here, the matching pursuit and simulated annealing algorithms were tested. They were chosen since they are fast and can be easily adapted to the constraints of the problem. According to our results, MP shows worse behavior compared to simulated annealing, in the sense that at the end, the configuration suggested by simulated annealing results in a better reproduction of the desired field than the one suggested by matching pursuit. However, if only a part of the mirrors can be used, and the rest can be turned off, the performance of MP is acceptable and it turns out to be stable for different types of fields. On the other hand, the simulated annealing algorithm, with its low computational complexity, exhibits a strong potential to produce good results when it is supplied with good initial conditions. However, at the moment, we are neither aware of systematic approaches for examining, assessing and speculating on the prospective impact of initial conditions to the final result of the algorithm, nor on ways of producing such good initial estimates. These problems must be undertaken in future works.

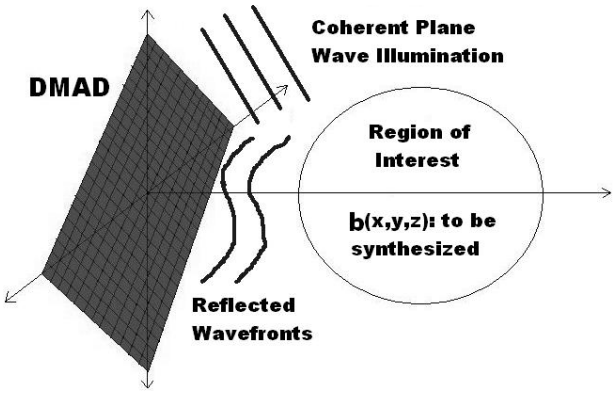

Figure 1. Light field synthesis with a DMAD

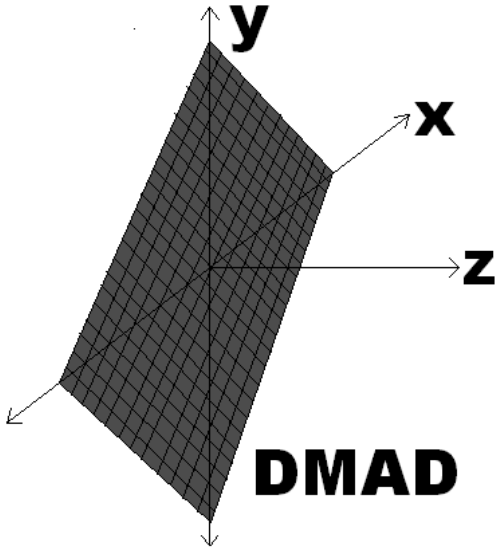

Figure 2. Chosen coordinate system

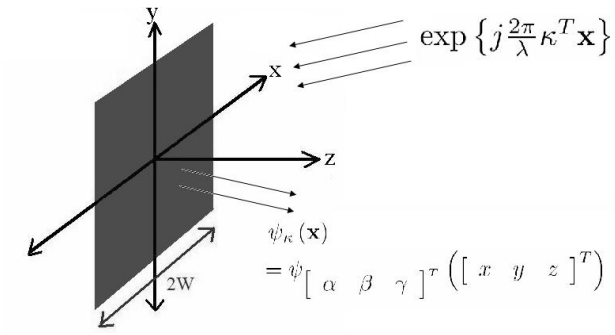

Figure 3. Physical interpretation of $\psi_\kappa(\mathbf{x})$ of Eq. 5

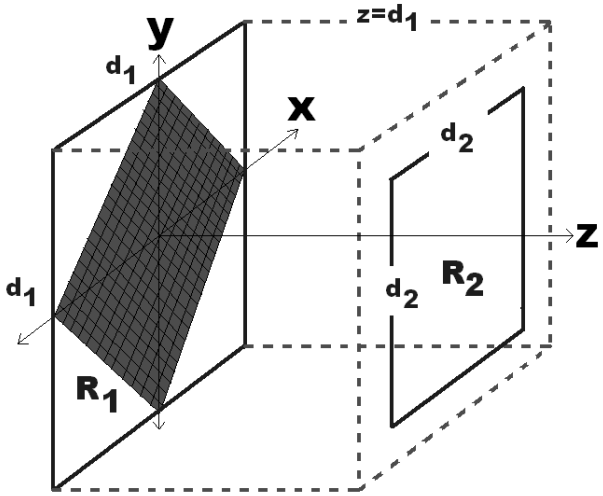

Figure 4. Placement of sampling patch with respect to DMAD

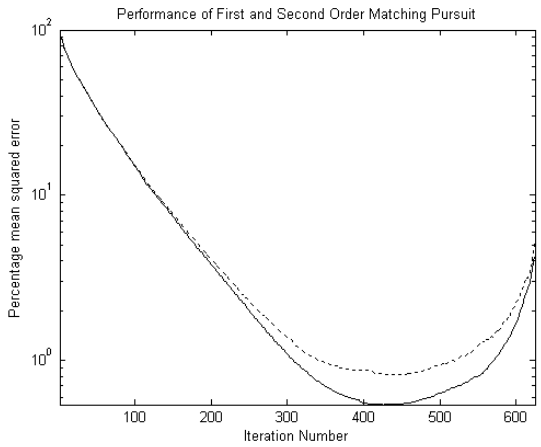

Figure 5. Error of first and second-order MP for field in range space

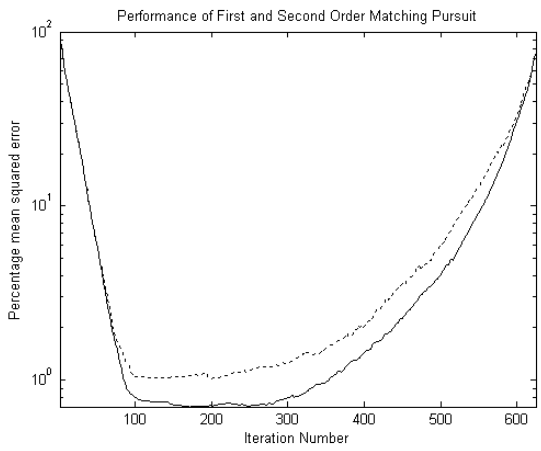

Figure 6. Error of first and second-order MP for circular field

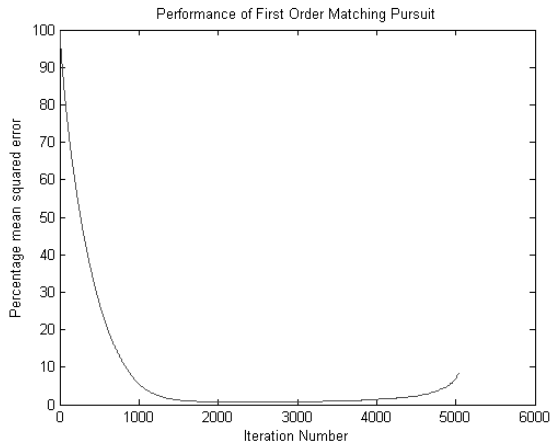

Figure 7. Error of first-order MP for field in range space

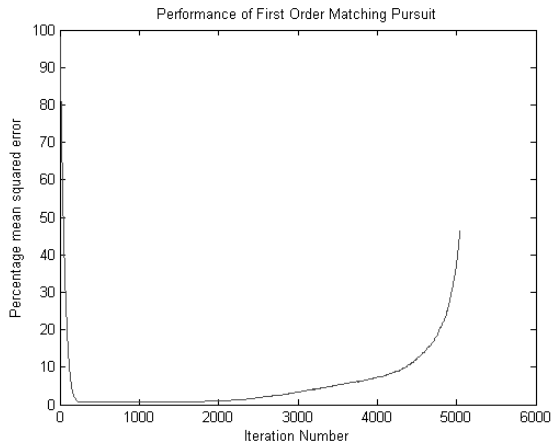

Figure 8. Error of first-order MP for circular field

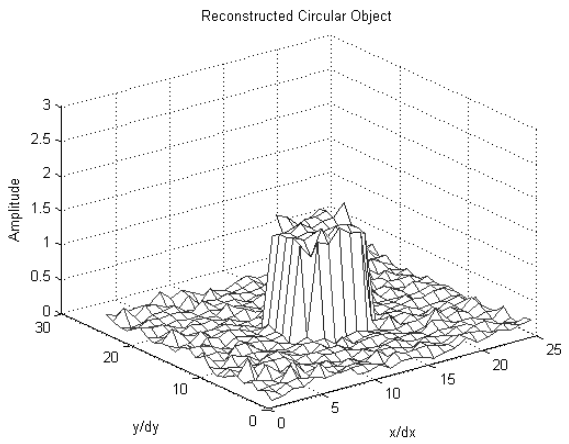

Figure 9. Reconstruction of circular object with simulated annealing

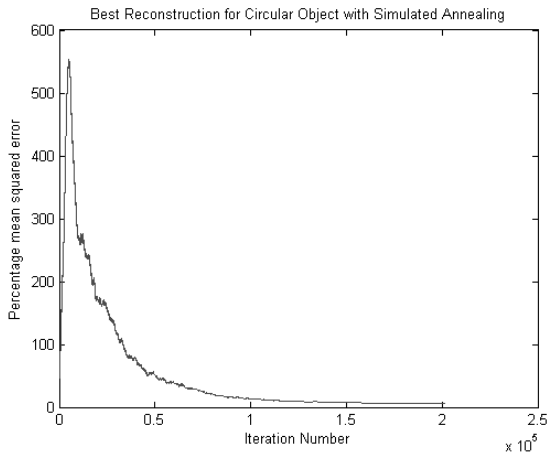

Figure 10. Error of simulated annealing for circular field

REFERENCES

1. R. J. Gove, "DMD display systems: the impact of an all digital display," in *Int Symp Society for Information Display*, Texas Instruments White Pages, 1994.
2. L. J. Hornbeck, "Digital light processing update: status and future applications," in *Conf on Projection Displays V, Proc SPIE*, **3634**, pp. 158–170, 1999.
3. R. S. Nesbitt, S. L. Smith, R. A. Molnar, and S. A. Benton, "Holographic recording using a digital micromirror device," in *Conf on Practical Holography XIII, Proc SPIE*, S. A. Benton, ed., **3637**, pp. 12–20, 1999.
4. T. Kreis, P. Aswendt, and R. Hofling, "Hologram reconstruction using a digital micromirror device," *Optical Engineering* **40**, pp. 926–933, 2001.
5. R. Piestun and J. Shamir, "Synthesis of three-dimensional light fields and applications," *Proceedings of the IEEE* **90**, pp. 222–244, 2002.
6. S. Kirkpatrick, C. D. Gelatt, and M. P. Vecchi, "Optimization by simulated annealing," *Science* **220**, pp. 671–681, 1983.
7. P. J. M. V. Laarhoven and E. H. L. Aarts, *Simulated annealing: theory and applications*, D. Reidel, 1987.
8. S. Mallat and Z. Zhang, "Matching pursuit with time-frequency dictionaries," *IEEE Transactions on Signal Processing* **41**, pp. 3397–3415, 1993.
9. E. Ulusoy, L. Onural, and H. M. Ozaktas, "Analysis of the complex light field generated by a deflectable mirror array device," in *International Conference on Holography, Optical Recording and Processing of Information*, (Varna, Bulgaria), 2005. to appear in Proc SPIE.
10. J. W. Goodman, *Introduction to Fourier Optics*, Mc-Graw-Hill, New York, 1996.
11. L. Onural, "Sampling of the diffraction field," *Applied Optics* **39**, pp. 5929–5935, 2000.
12. F. Gori, "Fresnel transform and sampling theorem," *Optics Communications* **39**, pp. 293–297, 1981.